GENERATION OF AN ADVANCED HELICOPTER EXPERIMENTAL AERODYNAMIC DATABASE

- THE WIND TUNNEL TEST OF THE EU-PROJECT GOAHEAD -

M. Raffel[1], F. de Gregorio[2], W. Sheng[3], G. Gibertini[4], A. Seraudie[5], K. de Groot[6], B.G. van der Wall[7]

1 German Aerospace Center (DLR), Aerodynamic and Flow Technology, Bunsenstraße 10, 37073 Goettingen, Germany
2 Centro Italiano Ricerche Aerospaziali (CIRA), Via Maiorise, 81043 Capua (CE), Italy
3 Department of Aerospace Engineering, University of Glasgow, University Avenue, Glasgow G12 8QQ, Scotland
4 Politecnico di Milano - Dipartimento di Ingegneria Aerospaziale, Via La Masa 34, 20156 Milano, Italy
5 ONERA, Aerodynamics and Energetics Model Department, B.P. 4025 2, av. E. Belin, 31055 Toulouse Cedex 4, France
6 German Aerospace Center (DLR), Aerodynamic and Flow Technology, Lilienthalplatz 7, 38022 Braunschweig, Germany
7 German Aerospace Center (DLR), Flight Systems, Lilienthalplatz 7, 38022 Braunschweig, Germany

Abstract

The GOAHEAD-consortium was created in the frame of an EU-project in order to create an experimental database for the validation of 3D-CFD and comprehensive aeromechanics methods for the prediction of unsteady viscous flows including rotor dynamics for complete helicopter configurations, i.e. main rotor – fuselage – tail rotor configurations with emphasis on viscous phenomena like flow separation and transition from laminar to turbulent flow. The wind tunnel experiments have been performed during two weeks in the DNW-LLF on a Mach-scaled model of a modern transport helicopter consisting of the main rotor, the fuselage, control surfaces and the tail rotor. Therefore, a closed test section has been used. The measurement comprised global forces of the main rotor and the fuselage, steady and unsteady pressures, transition positions, stream lines, position of flow separation, velocity profiles at the test section inlet, velocity fields in the model wake, vortex trajectories and elastic deformations of the main and tail rotor blades.

1. INTRODUCTION

During the past decade considerable progress has been made in developing aerodynamic prediction capabilities for isolated helicopter components. The isolated main rotor downwash structure has mainly been investigated by means of optical methods in hover flight conditions (e.g.[Heineck et al. 2000], [Martin et al. 2002]) or in wind tunnels on an isolated fuselages (e.g. [Raffel et al. 1998], [Murashige et al. 2000], [van der Wall & Richard 2006]). Today leading edge CFD software systems are available, and others are being developed, which are capable of predicting the viscous flow around main rotor-fuselage configurations or even complete helicopters. The greatest shortcoming for qualifying these methods as design tools in the industrial design process is the lack of detailed experimental validation data for the aerodynamics of complete helicopters. To overcome this shortcoming, the GOAHEAD-consortium (five national research centres, four universities, four helicopter manufacturers and one SME) was created in the frame of an EU-project in order to create an experimental database for the validation of 3D-CFD and comprehensive aeromechanics methods for the prediction of unsteady viscous flows including rotor dynamics for complete helicopter configurations, i.e. main rotor – fuselage – tail rotor configurations with emphasis on viscous phenomena like flow separation and transition from laminar to turbulent flow. The wind tunnel experiments have been performed during two weeks in spring 2008 in the DNW-LLF on a Mach scaled model of a modern transport helicopter consisting of the main rotor (R=2.1m), the fuselage (including all control surfaces) and the tail rotor. Clear boundary conditions were found to be of higher importance than wind tunnel simulations as close as possible to free flight. Therefore, the 6m x 8m closed test section has been used. Velocity profiles have been measured at the inflow plane in order to define accurate boundary conditions in the CFD simulations by means of hot-wire anemometry and wall pressures by means of pressure taps at the wind tunnel walls. The measurement comprised global forces of the main rotor and the fuselage, steady and unsteady pressures, transition positions, stream lines, position of flow separation, velocity fields in the wake, vortex trajectories and elastic deformations of the main and tail rotor blades.

TC	M_{WT}	M_{MR}	M_{TR}
1.1	0.059	0.617	0.563
1.2	0.204	0.617	0.563
1.3	0.259	0.617	0.563
2	0.059	0.617	0.563
3/4	0.204	0.617	0.563
5	0.259	0.617	0.563
6	0.280	0.617	0.563

Table 1: Executed Test Matrix

2. LIST OF SYMBOLS

Ω	Rotor rotational frequency, rad/s
ρ	Air density, kg/m³
a	Speed of sound, m/s
c	Blade chord, m
R	Blade radius, m
f	Effective fuselage drag area, m²
N_b	Number of blades
T	Rotor Thrust, N
W	Virtual model weight, N
Fx	Propulsive force, pos. forward, N
M_{WT}	Mach number of wind tunnel flow, $M_{WT} = V_{WT}/a$
M_{MR}	Mach number of blade tip in hover, main rotor,
M_{MR}	$= (\Omega R)_{MR}/a$
M_{TR}	Mach number of blade tip in hover, tail rotor,
M_{TR}	$= (\Omega R)_{TR}/a$
C_W/σ	Spec. weight coeff., $C_W/\sigma = W/[\rho N_b c R(\Omega R)^2]_{MR}$
CxS	Prop. force coefficient, $CxS = Fx/(\rho V^2_{WT} f/2)$
C_{TTR}/σ_{TR}	Tail rot. thrust, $C_{TTR}/\sigma_{TR} = T_{TR}/[\rho N_b c R(\Omega R)^2]_{TR}$
α_S	Rotor shaft angle of attack
α_{fus}	Fuselage angle of attack
Θ_{07}	Collective control angle, main rotor
Θ_C, Θ_S	Cyclic control angles
Θ_{TR}	Collective control angle, tail rotor

3. EXECUTED TEST MATRIX

The executed test matrix is summarized in table 1: TC 1 represents measurements of the isolated fuselage over a wide range of shaft angles with rotating stubs on the hubs in order to get the fuselage polars as well as the hub tare loads for the following test cases:

TC 1.1 – polar for TC 2 (pitch-up)

TC 1.2 – polar for TC 3 (cruise) and TC4 (tail shake)

TC 1.3 – polar for TC 5 (dynamic stall)

TC 1.4 – polar for TC 6 (high speed)

At the nominal conditions (predicted by the Eurocopter HOST code) a sensitivity study was performed to evaluate the effect of different control settings (collective and cyclic) on the hub tare loads. TC 2 – TC 6 are with rotor blades on the hubs.

TC 2 (pitch-up): The correct shaft angle setting must be identified during the test based on analysis of the dynamic content of the stabilizer leading edge dynamic pressure sensors as well on the dynamic content of the stabilizer balance. For this, a range of shaft angles was measured around the HOST prediction. Large vibrations were present at this low speed as expected in this configuration.

TC 3 (cruise): All parameters were pre-defined by the HOST prediction. Performed as prescribed, with low vibration.

TC 4 (tail shake): The correct shaft angle setting must be identified during the test based on analysis of the dynamic content of the fin leading edge dynamic pressure sensors as well on the dynamic content of the fuselage balance. For this, a range of shaft angles was measured around the HOST prediction, which was identical to TC 3. After investigation of data TC 3 was selected as condition for TC 4 as well.

TC 5 (dynamic stall): The HOST prediction was very close to the maximum available power provided by the model. Since the condition was declared as critical with high loads for all components of the model, the definition of the TC 5 case was kept open to the limits of the model experienced during the test. However, the wind tunnel and rotor tip speed Mach numbers are fixed, but allowance was given to modify the trim parameters. The goal was to come as close as possible to the high thrust level, while the shaft angle, propulsive force were free to be varied. Power, vibration, control and actuator force limits were reached. This was then selected as the dynamic stall case, which showed a pitch link force spike in the third quarter of the revolution – an indicator for stall inception.

TC 6 (high speed): A high advancing blade tip Mach number of 0.91 was envisaged here with reduced stall, thus an increased tip Mach number was chosen. Again, large dynamic loads and rotor power were expected. Therefore, as in TC 5, the actual trim settings were left open according to the limits encountered during testing. Power and control limits were reached. This was selected finally as the high speed case, leading to a tip Mach number of the advancing blade of 0.897.

All pressure, SPR, SPA, PIV etc. measurements were then performed with continuous repeats of these conditions. It was found that a very good repeatability was present of the trim and balance data throughout the rest of the test.

4. FUSELAGE THERMOGRAPHY

DLR has been responsible for the detection of the laminar-turbulent transition on the fuselage of the model with infrared thermography. For the infrared measurements two infrared cameras have been used, one for the side view and another one for the top view of the model fuselage. The cameras have been installed at an appropriate position near the tunnel wall behind special orifices in the tunnel wall. Since the DNW-LLF is an atmospheric wind tunnel no special infrared windows were required. The camera for the side view has been mounted with a 10° lens on a special displacement unit, which allowed an adjustment of the view from the infrared computer via remote control and more than one measurement at a data point at different regions of the model. The camera for the top view has been mounted with a 20° lens on a tripod head allowing an exact adjustment of the upper region of interest. The cameras used were FLIR System SC3000 cameras with a GaAs QWIP chip (Quantum Wall Infrared Photo detector), Cooled down to 70 K by liquid nitrogen operated at 50 frames/s (with averaging). Since the GOAHEAD model fuselage had been constructed from CFK, no modification for the infrared measurements was necessary. A clear detection of the laminar-turbulent transition requires a small difference in the temperature (some Kelvin) of the model and the incoming flow in order to generate heat transfer. At high Mach numbers this temperature step could be achieved by warming up the model with the frictional heat of the flow and additionally switching the cooler of the wind tunnel for a short time off. Two special infrared radiators have been installed in the nose of the GOAHEAD model. The radiators, with a maximum power of 500W each, have been supplied with a regulated power supply. A small fraction of this power for only short periods of time was necessary for sufficient temperature steps in order to perform adequate infrared measurements. In the frame of the GOAHEAD wind tunnel test, infrared measurements have been performed during three days at 164 data points. A complete set of the results measurements has been placed in the data base. Some typical infrared image, sampled at different conditions, are shown and discussed in the following.

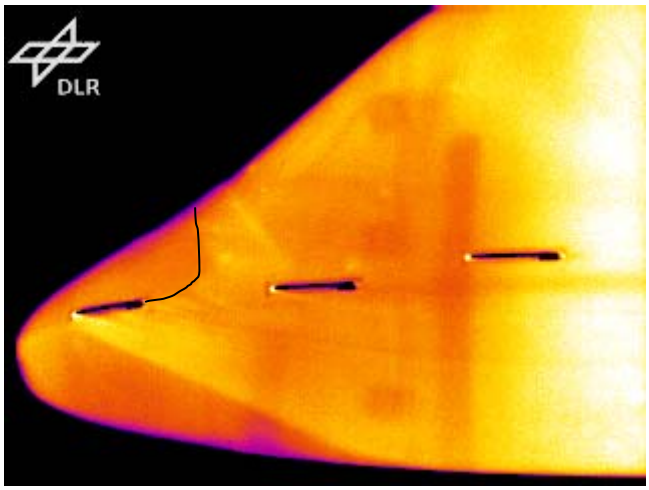

Figure 1: Infrared image of data point 185 (side view) of the front part of the fuselage at **Ma 0.259** and **α = -1°.**

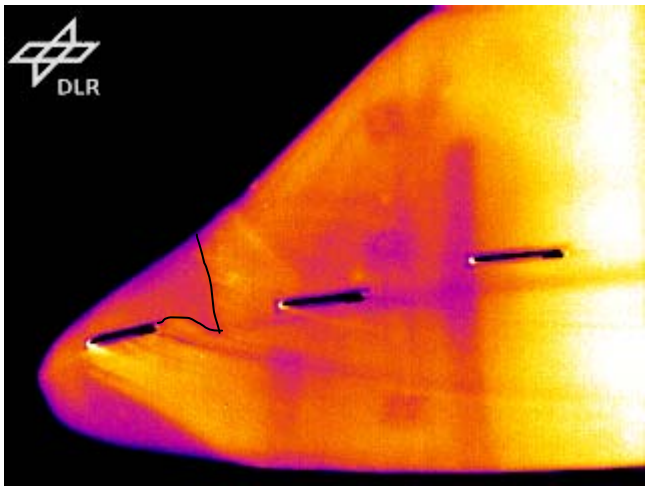

Figure 2: Infrared image of data point 183 (side view) of the front part of the fuselage at **Ma 0.259** and **α = -5°.**

The infrared images of the side view for the dynamic stall measurements at Ma 0.259 are shown in the figures 1 and 2 for two different angles of attack. The laminar-turbulent transition (see the black lines as a guide to the eye) at this Mach number was considerably far upstream and the first hot film now act completely as tripping device for the laminar flow at the nose.

The infrared measurements have shown that infrared thermography for helicopter models delivered adequate two-dimensional information of the boundary layer state. With this technique, remarkable areas with laminar flow especially at the nose at all angles of attack and also at the bottom and at the side part of the fuselage at higher angles could be detected. The other installed camera for the top view has delivered additional information. Free transition could be found at the upper side of the nose at higher speeds (cruise speed and dynamic stall) and higher angles of attack. At low speed (pitch up) and lower angles of attack the transition is mainly forced by the pressure rise at the bend between the nose and the window and the bend in the side part. The free or forced transition at the side part of the fuselage could not be clearly detected due to the disturbances of the mounted hot films and especially their soldering points. As expected, the infrared heating inside the model lead to infrared images with higher contrast to detect the laminar-turbulent transition but also measurements

without this heating lead to sufficient image quality.

5. INFLOW HOTWIRE MEASUREMENTS

In order to provide information about inlet flow and, in particular, in order to verify whether the turning rotor did influence the inflow condition, some flow surveys have been carried out at the test section inlet by means of triple hot film probes. The choice of hot films instead of classical thinner hot wires was due to the need of robustness although these kind of probes produces, in our experience, a distortion of the turbulence spectrum usually resulting in an overestimation of turbulence level. A calibration was carried out in laboratory where a correction law has been found by comparison with hot wire probe spectrum in order to correct for this effect. The probe was calibrated with respect to Reynolds number and velocity direction at Politecnico di Milano aerodynamic laboratory under monitored conditions. The calibration procedure took the effects of physical conditions (temperature, pressure and humidity) into account so that the calibration itself could be extended to different conditions [Durst et al. 1998]. Two triple hot-film probes have been used during the tests, kept in the required positions by a double-prong sting mounted on a heavy strut. The sting was provided with a two-component inclinometer in order to correct for possible bending due to aerodynamic loads. The distance between the two probes was 200mm. Due to the test section size, the probes were connected to the control unit by means of long cables (15m) and thus six apposite resistances, each one equivalent to the corresponding cable and wire, had to be supplied to the system in order to balance the Wheatstone bridges. The six signals from the two probes were simultaneously acquired at 150 kHz and filtered with six 8-pole Butterworth low-pass filters with 50 kHz cut-off frequency. The probes were positioned in 9 different positions at inlet section to get a first estimate of the inflow conditions. The turbulence energy was essentially unaffected by the rotors action as similar low values, in the order of $2*10^{-2}$ m^2s^{-2} were found with and without the rotors. The values of the measured deflection were in the order of one tenth of degree or less and the speed difference less then 0.5 % Thus, they are quite small differences indeed and inside the accuracy of the measurement technique [Maciel et al. 2000]. The turbulence was anisotropic with lower intensity in the stream-wise direction due to the contraction effect [Han et al. 2005]. Figure 3 shows a comparison between spectra obtained on the centre of inlet section with and without rotors: disturbances due to rotors are clearly recognizable in the corresponding spectrum but their contribution to the total turbulence energy is negligible.

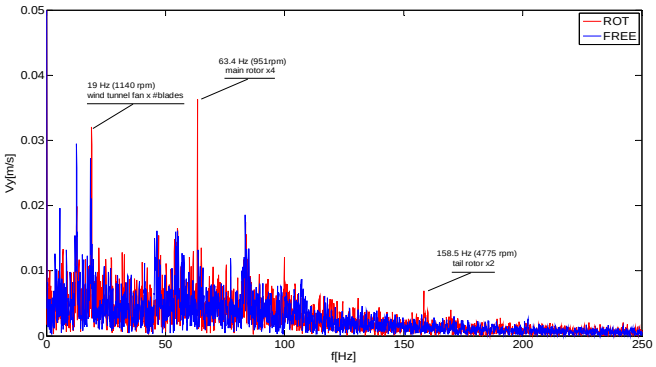

Figure 3: Measured in-flow velocity fluctuations over the frequency

6. RESSURE MEASUREMENTS

Steady and unsteady pressures have been measured on the fuselage by 292 pressure taps and 130 unsteady pressure transducers.

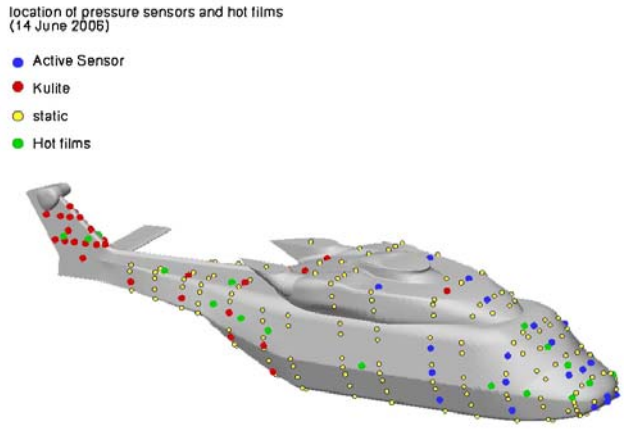

Figure 4: Pressure taps (static-yellow) and unsteady sensors (unsteady- blue and red)

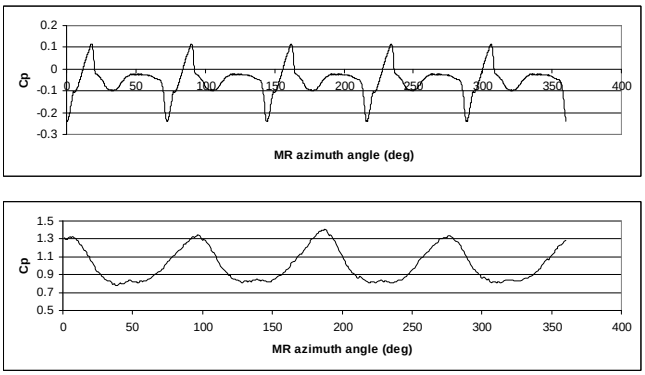

Figure 5 and 6: Nose pressure history at M=0.059

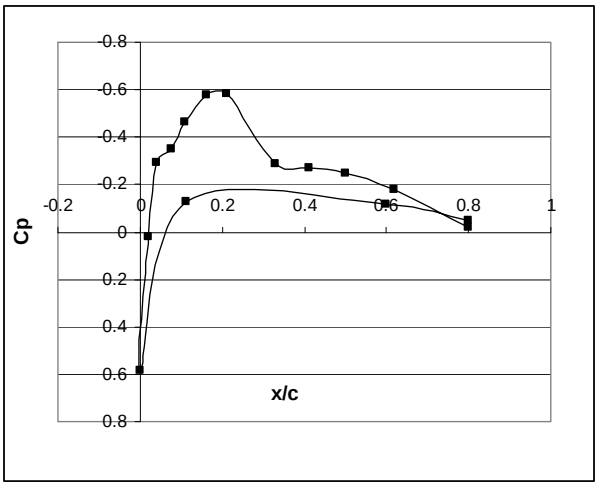

Figure 7: Pressure distributions at 82.5% spanwise (Main rotor, M=0.204) at ψTR=90°

Unsteady pressure data on fuselage have been recorded for isolated helicopter model in three different Mach numbers (M=0.059, 0.204 and 0.259), and the complete helicopter model in four Mach numbers (M=0.059, 0.204, 0.259 and 0.280). The figure below shows the results of pressure signals on helicopter nose at M=0.059 (complete helicopter model).

Additionally, 118 unsteady pressure sensors were installed on the main rotor, distributed on 4 rotor blades, including five sections on 3 rotor blades (spanwise at 97.5%, 91.5%, 82.5%, 70% and 50%), and 16 sensors were installed on Blade 4 at the leading edge region (2%c upper and lower surfaces) in 8 sections (95.25%, 90%, 87.5%, 85%, 80%, 75%, 60 % and 40%).

14 sensors were distributed on each of two sections (spanwise: 80% and 97%), and 8 sensors at the leading edge (3%c upper and lower surface) on 4 spanwise positions: 50%, 60%, 70%, and 90. The unsteady pressure data on main rotor have been recorded for the complete helicopter model, including four different Mach numbers (M=0.059, 0.204, 0.259, and 0.280).

Unsteady pressure data on main rotor have been recorded for the complete helicopter model, including four different Mach numbers.

7. BLADE HOTFILM MEASUREMENTS

In order to determine the boundary state on the blades, hot films were glued on 4 sections for the wind tunnel tests. Hot film arrays from TAO Systems were implemented and conditioned with units specially designed and manufactured by ONERA. Despite the lack of useful sensors on the blades (9 over 40), the available signals have been analyzed for the tested configurations (TC2 to TC6). An attempt was made to evaluate the boundary layer state in the cruise condition case (TC3-4), at M = 0.204. The analysis of hot film signals was done computing the mean and RMS values with a phase average method. A typical mean value signal (X/C = 14%) is plotted versus the rotor azimuthal angle in figure 8: the abrupt increase of the level corresponds to a change from laminar to a turbulent boundary layer state, a sudden decrease illustrates a change from a turbulent to a laminar state. The RMS values exhibit peaks for each abrupt evolution of the mean level. From this analysis, a state of the boundary layer is proposed for this location (X/C = 14%) and 2 spanwise sections (Y/L = 60 % blade 3 and 80 % blade1) in figure 3.

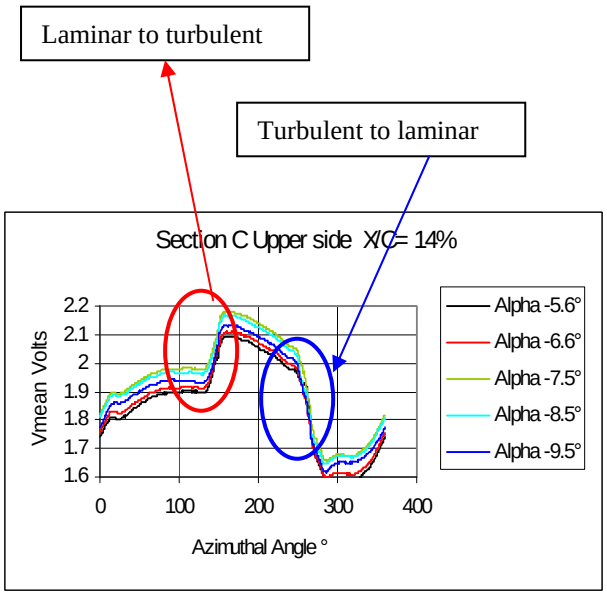

Figure 9: Hotfilm signals evolution in a rotor cycle

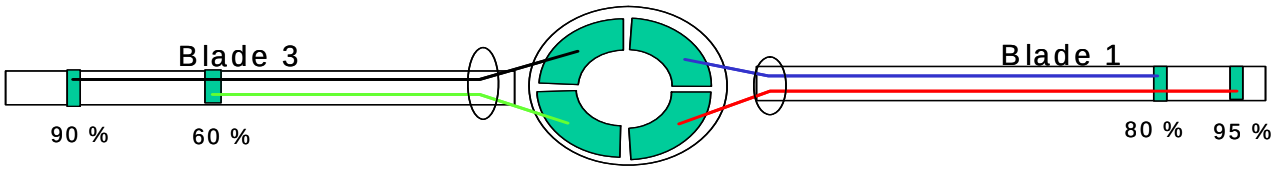

Figure 8: Hotfilm locations on main rotor

Along the rotor cycle, blue parts represent the laminar regions, red parts the turbulent ones; grey regions of the diagram are relative to separated zones. This boundary layer state is valid for the leading edge part of the blades (0%<X/C<14%); further downstream, a monotonous evolution of the mean level is provided by the sensors due to a turbulent state of the boundary layer.

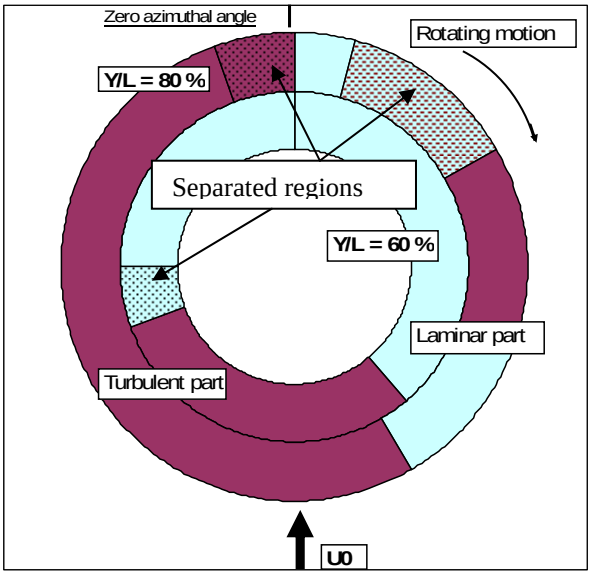

Figure 10: TC3-4 boundary layer state at X/C=14 %

8. PIV VELOCITY MEASUREMENTS

PIV measurements have been performed as well on the isolated fuselage (see figure 11) as on the full helicopter model for different flight conditions by CIRA, DLR and DNW. The flow region downstream the rotating hub and downstream the rear hatch of the helicopter model has been investigated for flight cruise condition (TC3-4). Three components PIV measurements have been carried out in phase with the main rotor azimuth angle on several cross planes downstream the rotating hub (Flow region PIV1). For each cross plane five different azimuth angle positions have been investigated (ΨMR=0°, 22.5°, 45°, 67.5° and 90°). The sample files presented below (figure 11 and 12) show the wake flow behind the rotating hub, for the cases of isolated fuselage (test condition TC1) and full model (test condition TC3-4). The pictures show the mean phase locked velocity field for the main rotor azimuth angle of 0°, the velocity magnitude is shown colour coded together with streamline computations.

Analogous for flight cruise condition, the flow field region downstream the rear hatch of the fuselage has been characterised by measuring the three velocity components on several cross planes (flow region PIV2) synchronizing the measurement system with the rotor azimuth position of ΨMR=0°.

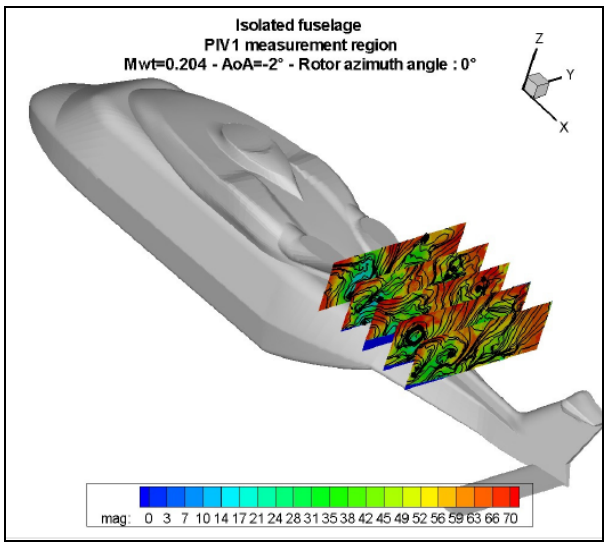

Figure11: TC1 – PIV1 - Isolated fuselage ΨMR=0°

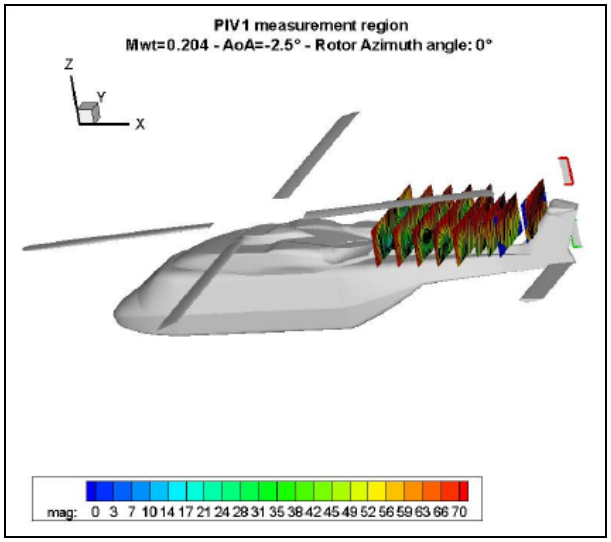

Figure12: TC3-4 –PIV1 -Full model for ΨMR=0°

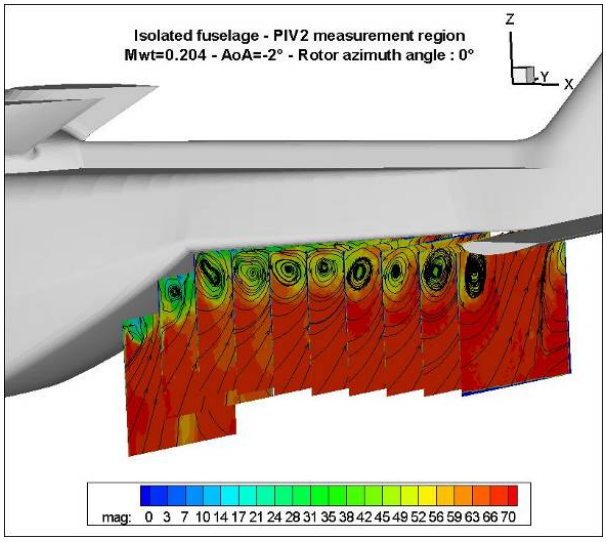

Figure13: TC1 – PIV2 isolated fuselage for ΨMR=0°

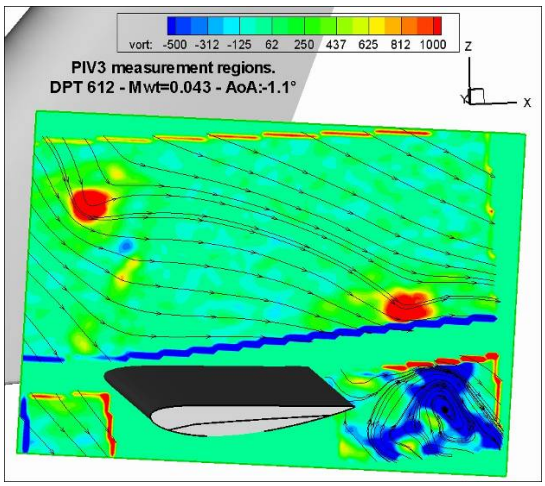

Figure 15: TC2 – PIV3 full model ΨMR=142.6°

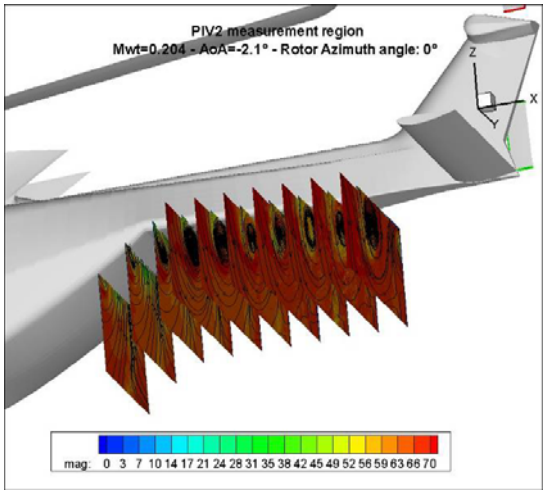

Figure 14: TC3-4 - PIV2 Full model for ΨMR=0°

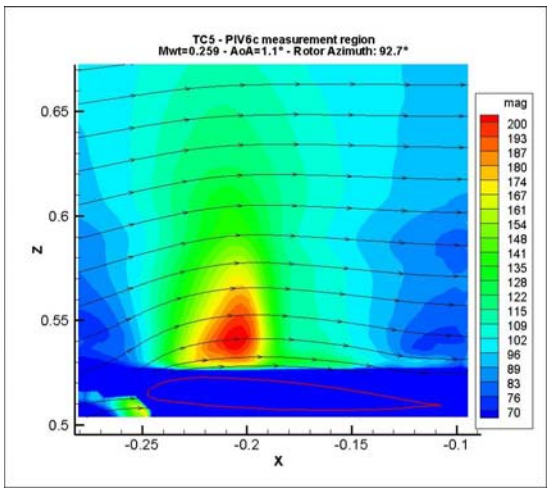

Figure 16: Advancing blade ΨMR=90°

The figures 13 and 14 clearly show two counter rotating vortices shedding by the lower region of the fuselage and their position moving downward.

The pitch up flow condition (test condition TC2) has been investigated measuring the flow field behaviour on a vertical longitudinal plane above the horizontal stabilizer (flow region PIV3). In Figure 15 the orthogonal component of the vorticity is shown colour coded together with streamline computations. Two vortices coming from the tip rotor blades are clearly visible above the horizontal tail plane and a strong circulation region due to flow separation is detected downstream the stabilizer.

In addition to the larger observation areas in the near and far wake of the helicopter model two close up recording areas in the proximity of the rotating main rotor blades where chosen: The tip region of the advancing blade (shown in figure 16), a flow field with embedded shock waves, and the flow field above the retreating blade at high flight velocities characterized by dynamic stall (sample figure 17 below).

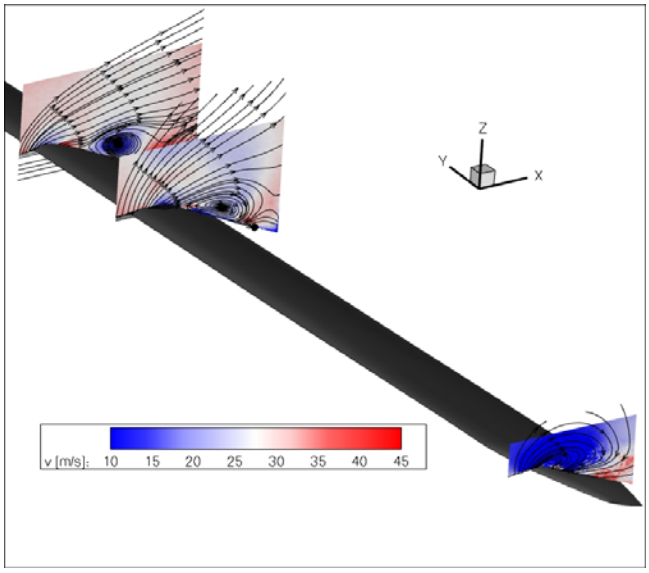

Figure 17: Dynamic stall PIV measurement results at the retreating blade ΨMR=270°

9. CONCLUSIONS

The flow field in the vicinity of a fully equipped helicopter rotor model has been investigated by means of unsteady and steady pressure transducers, infrared imaging, hot wire and hot film anemometry and particle image velocimetry. The results have been used in order to fill a meaningful database for helicopter CFD code validation. Although, the large-scale application of optical testing methods and the traversing of laser and camera equipment was hampered by the closed wind tunnel test section a quite complete set of experimental data could be sampled and is now ready to be used.

10. ACKNOLEDGEMENTS

The authors very much appreciate the cooperation with all participating partners, the EU and the wind tunnel staff of DNW-LLF.

11. REFERENCES

[Durst, et al. 1998] F. Durst, S. Noppenberger, M. Still, H. Venzke, Influence of humidity on hot-wire measurements, Meas.Sci.Technol., vol.7, pp.1517-1528, 1996.

[Maciel et al. 2000] Y.Maciel, C. Gleyzes, Survey of multi-wire probe data processing techniques and efficient processing of four-wire probe velocity measurements in turbulent flows, Experiments in Fluids, vol. 29, pp.66-78, 2000.

[Han et al. 2005] Y. O. Han, W. K. George, J. Hjarne, Effect of a Contraction on Turbulence. Part 1: Experiment, AIAA 2005-1119, 2005.

[Heineck et al. 2000] J. T. Heineck , G. K. Yamauchi, A. J. Woodcock, L. Lourenco, Application of three-component PIV to a Hovering Rotor Wake. 56th annual forum of the American helicopter society, Virginia Beach, VA, USA, 2000.

[Martin et al. 2002] P. B. Martin, G. J. Leishmann, Trailing vortex measurements in the wake of a hovering rotor blade with various tip shapes. 58th annual forum of the American helicopter society, Montreal, Canada, 2002.

[Murashige et al. 2000] A. Murashige, N. Kobiki, A. Tsuchihashi, H. Nakamura, K. Inagaki, E. Yamakawa, ATIC Aeroacoustic Model Rotor Test at DNW. 24th European rotorcraft forum, Marseille, France, 2000.

[Raffel et al. 1998] M. Raffel, U. Seelhorst, C. Willert, Vortical flow structures at a helicopter rotor model measured by LDV and PIV. Aeronautical Journal, The Aeronautical Scociety, 102 (1012), 221-2276, 1998.

[van der Wall & Richard 2006] B. G. van der Wall, H. Richard, Analysis methodology for 3C-PIV data of rotary wing vortices, Experiments in Fluids, 40, 798-812, 2006.